CIVIL ENGINEERING JOURNAL

Article no. 30

THE CIVIL ENGINEERING JOURNAL 3-2025

CONSTRUCTION PROCESS ANALYSIS OF THE COMBINATION SYSTEM BRIDGE OF CABLE-STAYED BRIDGE AND SHAPED ARCH BRIDGE

Jianwei Li, Hongjian Lu and Wentao Xu

Puyang Institute of Technology, Henan University, West Section of Yellow River Road, Puyang, Henan Province, China; pygxyljw@163.com

Received: 30.01.2025
Received in revised form: 14.07.2025
Accepted: 30.08.2025

ABSTRACT

The combination system bridges of cable-stayed and shaped arch bridges feature innovative structures and complex force distributions, necessitating intricate construction processes. Monitoring these processes ensures that the bridge's stress state aligns with designed internal forces. Measured stress values on the main girder's edges align with theoretical trends but are slightly lower. Throughout construction, the middle span experiences compression, with maximum stresses of -5.1 MPa on both edges. Full support during construction minimizes the impact of stay cable and derrick tension on main girder stress. After support removal, compressive stress increases on the upper edge and decreases on the lower. The tower's elevation is slightly above design, aiding in reducing prestress loss and deflection in later stages. At 16.5 m above the bridge girder, the tower's left side experiences tension and the right compression, with a tensile stress of only 1.0 MPa, indicating sound design and effective construction control.

KEYWORDS

Combination system bridges of cable-stayed bridge and shaped arch bridge, Construction monitoring, Stress, Elevation

INTRODUCTION

The primary load-bearing components of a cable-stayed bridge comprise the stay cables, bridge tower, and stiffened girder [1]. During the early 20th century, significant advancements in the development, refinement, and manufacturing of high-strength, high-elastic steel wire, along with its corresponding anchor system, combined with enhancements in orthotropic steel deck panels, fuelled the rapid evolution of cable-stayed bridges [2,3]. However, as the spans of cable-stayed bridges have widened, ensuring the stability of the cantilever section of the stiffened girder prior to closure has grown increasingly complex. Notably, the axial force within the stiffened girder has surged, leading to an elevated proportion of dead weight. Consequently, the height of the bridge tower has increased, and the sag effect of the stay cables has become more pronounced [4].

The arch bridge, as one of the foundational types of bridges, boasts a historical legacy stretching over 3,000 years. Over this extended period, continuous innovations in construction materials, technology, and design theory have evolved arch bridges from ancient stone structures dating back to pre-Christian times, through the concrete and simple steel arch bridges of the 19th century, to the

advanced truss arch and concrete-filled steel tube (CFST) arch bridges of the 20th century [5-7]. Presently, significant breakthroughs have been achieved in both the span and structural configurations of arch bridges. However, as spans increase, so do the dead loads of traditional arch bridges, thereby escalating the challenges associated with cable construction. Additionally, CFST arch bridges face issues such as susceptibility to corrosion and void formation within the concrete fill. Steel arch bridges, on the other hand, are marked by high construction costs, substantial maintenance expenses, and prominent stability concerns [8-10].

Cable-stayed bridges and arch bridges are currently utilized extensively worldwide; however, their inherent limitations hinder further advancements in bridge span capabilities [11-14]. In recent years, due to the escalating demand for aesthetic appeal in bridge design, the engineering community has proposed a hybrid system that combines cable-stayed and shaped arch bridges. This innovative bridge type capitalizes on the strengths of both cable-stayed and arch bridges while compensating for their respective shortcomings [15,16].

The composite system bridge not only enhances the spanning capacity and structural rigidity but also boasts a more visually appealing design. It improves the stability of the bridge structure, enhances safety during construction and operation, and reduces the height of the bridge tower. This bridge exhibits exceptional cooperative performance, mitigating tensile forces in stay cables or slings, facilitating a more uniform distribution of internal forces, minimizing local stresses, and offering superior structural performance along with substantial economic benefits [17-20].

The construction control technology of cable-stayed bridge, arch bridge, suspension bridge and continuous beam bridge has developed rapidly in China, but the research on the construction control of cable-stayed arch cooperative system bridge is relatively few, and the development of construction control is not very mature. On the basis of previous studies, this paper adopts adaptive control method to control the bridge construction.

PROJECT OVERVIEW

A combination system bridge of cable-stayed bridge and shaped arch bridge, with span arrangement of 40 m+90.5 m. The carriageway has a 1.5% transverse slope in both directions, and the sidewalk has a 1% transverse slope in one direction (inward). The main beam is a prestressed concrete cast-in-place box beam with a height of 2.7 m~3.8 m. The tower has a concrete section and is 59.5 m above the bridge girder. The distance of the stay cables is 8.5m, and there are 8 pairs of stay cables. The two arch ribs are constructed using a steel box structure, with concrete being poured only at the arch foot. The distance of the sling is 4.25 m, and there are 38 slings in the whole bridge. The bridge layout diagram is shown in Figure 1.

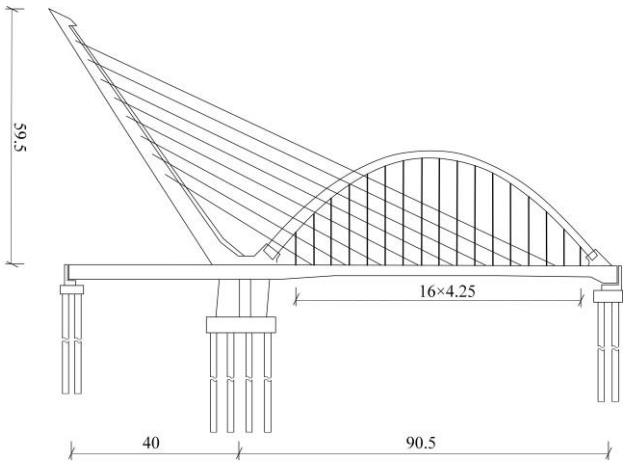

Fig.1- Schematic diagram of bridge layout（Unite: m）

Main girder

The main girder consists of a prestressed concrete cast-in-place box beam with a height of 2.7 m. Within a range of 21 m, the top of the pier transitions from 2.7 m in height on the left and right sides to 3.8 m. The main girder is provided with an end beam at 0# abutment with a width of 1.5 m. The top of 1# pier is provided with a middle beam, which is a box-type structure with a total width of 16.4 m, a middle web width of 3 m, and a web width of 0.8 m on both sides. An end beam is set at the 2# abutment. The beam retains its box-type structure, featuring an overall width of 5.5 m, a web width of 0.7 m, and a girder height of 3.8 m. A cross-sectional view of the bridge is depicted in Figure 2.

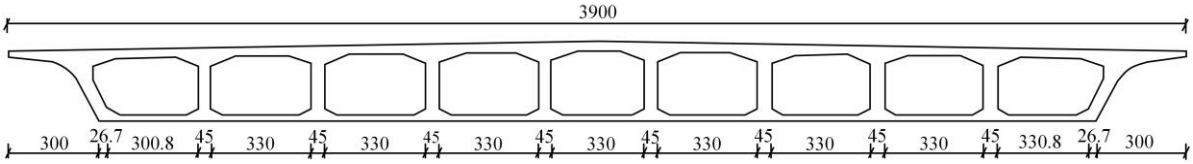

Fig. 2 - Cross section of the bridge (cm)

Tower

The bridge tower is constructed from reinforced concrete utilizing C50 concrete material. The portion of the tower situated above the bridge girder stands at a height of 59.5 m, with a horizontal inclination angle of 56° and a rear inclination angle of 34°. The tower section is rectangular in shape, featuring a transverse width of 3.5 m. The longitudinal width tapers from wider at the base to narrower at the top, with the longitudinal width at the tower top measuring 2.2 m. The base of the tower is widened to 6 m and is integrated with the main beam, arch, and pier for added stability.

Arch rib

The arch rib is constructed as a steel box structure, comprising two separate arch ribs, with concrete poured only in the vicinity of the arch foot. The span of each arch rib measures 84 m, and the ratio of the rise (vector) to the span is 1/3. Both ends of the arch rib feature concrete arch feet that are integrated with the main girder, tower, and pier. The arch rib extends deeply into the length of the concrete arch foot, and the interface between the arch foot and the concrete is connected using a pressure plate. To ensure seamless force transmission within the structure, the pressure plate is designed with a thickness of 60 mm.

Arch rib transverse wind bracing

Transverse steel arch rib is provided with 3 wind braces, wind braces into a "K" shape. The section forms of each main pole and strut are square. The main rod section size of the first two wind bracings is 60 mm×60 mm, and the section thickness is 10mm. The section size of the main rod of the third wind bracing is 80 mm × 80 mm, and the section thickness is 16mm. The section size of the strut of the wind bracing is 40 mm×40 mm, and the section thickness is 10mm.

Cable and sling

A total of 8 cables are arranged longitude wise, and the cable layout spacing is 8.5m. They are stretched on the tower and anchored on the girder. A total of 19 slings are arranged longitudinally in the arch rib slings, and the arrangement distance of the slings is 4.25 m. The slings are stretched on the bottom plate of the box girder, and the upper anchorage point is arranged outside the arch rib of the steel box with ear plates. Both the cable and the boom are made of steel strand cables, and the standard tensile strength is 1860MPa. The cable specifications are GJ15-25 and GJ15-31, which

are tensioned on the tower and anchored on the girder. The suspender specifications are GJ15-12, GJ15-17 and GJ15-19, which are stretched on the bottom plate of the box girder, and the upper anchorage point is arranged on the outer side of the arch rib of the steel box with ear plates.

BRIDGE CONSTRUCTION PROCESS AND SIMULATION

Construction process

The construction process of cable-stayed arch bridge is mainly divided into substructure construction, main girder construction, cable tower construction and stay cable tension, arch rib construction and suspender tension.

Main girder construction

The main girder was poured for the full support. The support was set up and pre-pressed to eliminate the inelastic compression of the support. The main concrete beam is poured in layers, the bottom plate is poured first, then the web is poured, and the roof is poured finally. The concrete parts of the two arch feet were poured together with the main beams.

Tower construction and cable tensioning

The portion of the tower situated above the bridge girder reaches a height of 59.5 m. The bridge tower boasts a tilt angle of 34°, and its cross-section is solid, with a transverse width of 3.5 m. The longitudinal width tapers from wider at the base to narrower at the top. The cable tower section below the main beam is poured together with the side pier. The cable tower section above the main beam is divided into two sections from the bottom up: rectangular solid prestressed section B and cable section A with large inclination rectangular section. The section A is divided into A1~A16 sections every 4m along the direction of the cable tower. Section B (0 m~6.6 m above the bridge girder) adopts the cast-in-place construction technology, section A1~A3 (6.6 m~20 m above the bridge girder) adopts the inverted mold construction method, and A4~A16 (20 m~59.5 m) adopts the inverted mold construction technology, as shown in Figures 3 and 4.

The cable-free area of the bridge tower is constructed by cast-in-place construction with supports, while the cable-supported area is constructed with climbing formwork. During the construction of the climbing formwork, when the bridge tower sections are anchored by the tension cables, the tension cables are initially tensioned to ensure that the initial tension force of the tension cables can balance the weight of the bridge tower.

All the sections of the tower are divided horizontally, and the construction phase is divided as shown in Figure 5. After the construction of the cable tower in section A6, the initial tension of the cable S01 is started. Then every construction of 1 to 2 sections of the tower will be initially stretched a cable. The cable is tensioned three times. After the tower is completed and the initial tensioning of the cable is completed, the cable is tensioned a third time.

Fig. 3 - Cable tower and arch rib support

Fig. 4- Tower turning mold construction

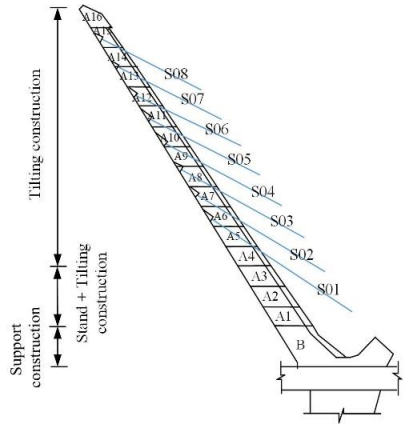

Fig.5 - Schematic diagram of tower construction phase division

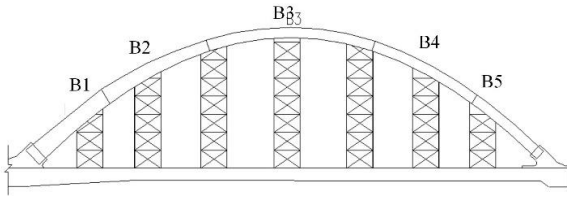

Fig.6 - Segment division of arch rib and support layout diagram

Arch rib construction and sling tension

Concrete arch foot is poured (poured together with the main girder concrete) and steel box arch is embedded in the arch foot section. Install the boom, stretch the boom in sections, and the tension sequence is as follows: D5, D9, D13, D8, D10, D4, D14, D1~D3, D6, D7, D11, D12 and D15~D17.

Construction simulation

The spatial model of the cable-stayed arch bridge was established by using Midas/Civil finite element software. The construction state of cable-stayed arch bridge is simulated, and the results of calculation and analysis are used to guide the construction control. The structure of the main bridge is divided into a spatial beam lattice system by static calculation. Beam elements are utilized for the main girder, main tower, and arch rib, while truss elements are employed for the stay cables and suspenders. The piers, towers, beams and arches are consolidated together, and the bottom of the piers is consolidated and constrained. Stay cables share nodes with towers and beams, and hangers share nodes with arches and beams. A diagram illustrating the structural dispersion is depicted in Figure 7.

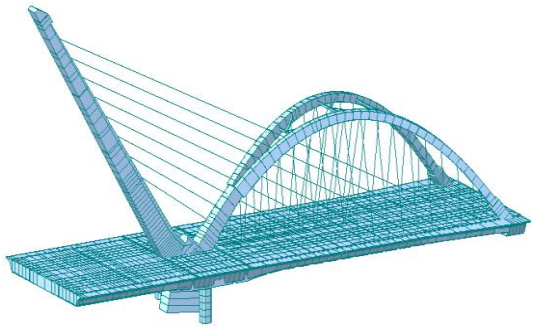

Fig. 7- Bridge finite element calculation model

BRIDGE CONSTRUCTION CONTROL CONTENT

The construction monitoring of cable-stayed arch bridge mainly adopts the adaptive control method, and the correction end point control method is adopted in some sections. According to the principle of controlling the linear shape and cable force value of the main girder, tower and arch rib, the stress control of the main girder, arch rib and tower is supplemented, the control section of the whole bridge is comprehensively monitored. The stress state of bridge structure in each construction

process should be mastered, and the stress, linear shape, displacement and reaction of each control part in each construction stage should be strictly controlled to ensure the structural safety in the construction process.

Structural stress and temperature field monitoring

The stress control section should be identified as the most disadvantageous (the most critical or disadvantageous point) of the main girder, crossbar beam, tower, arch rib, and cross brace during each construction stage or upon completion of the bridge. The precise arrangement of the monitoring sections is illustrated in Figure 8.

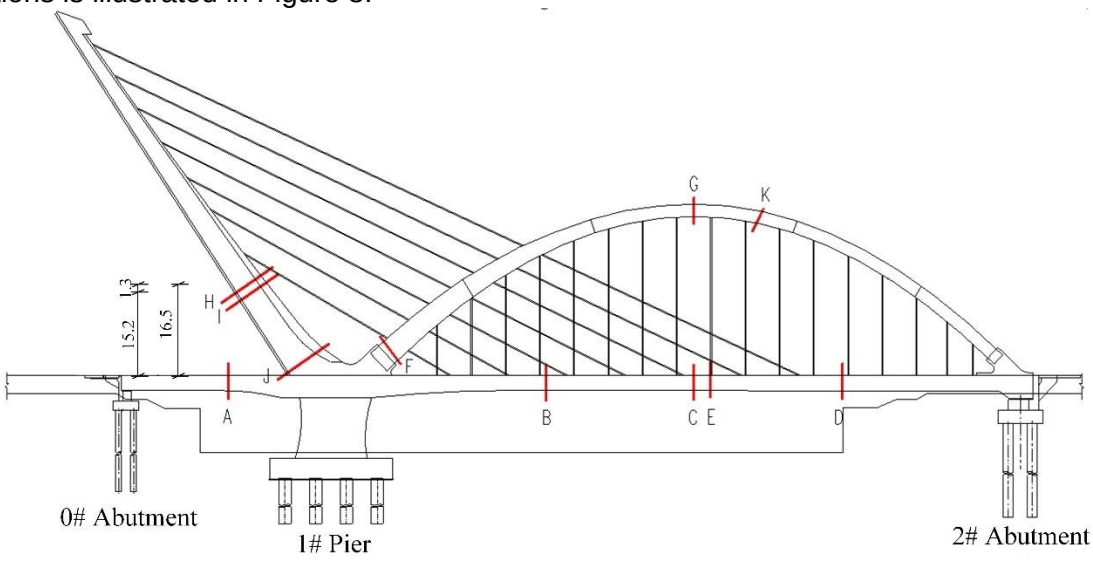

Fig.8 - Stress and temperature monitoring section layout (m)

Main girder and transverse spacer beam

Strain and temperature measurement points are strategically placed in various sections of the bridge, including the middle of the first span, the L/4 section of the second span, the L/2 section of the second span, and the 3L/4 section of the second span. Sections A, B, C, and E depicted in the figure correspond to the strain and temperature testing sections of the main beam. The strain sensors for the main beam should be installed along the longitudinal axis of the bridge. Specifically, a total of 16 strain gauges and 3 temperature sensors are installed on the main beam, while an additional 4 strain gauges bring the total to 20 strain gauges along with 3 temperature sensors on both the main girders and transverse beams. The arrangement of these measurement points is clearly shown in Figure 9.

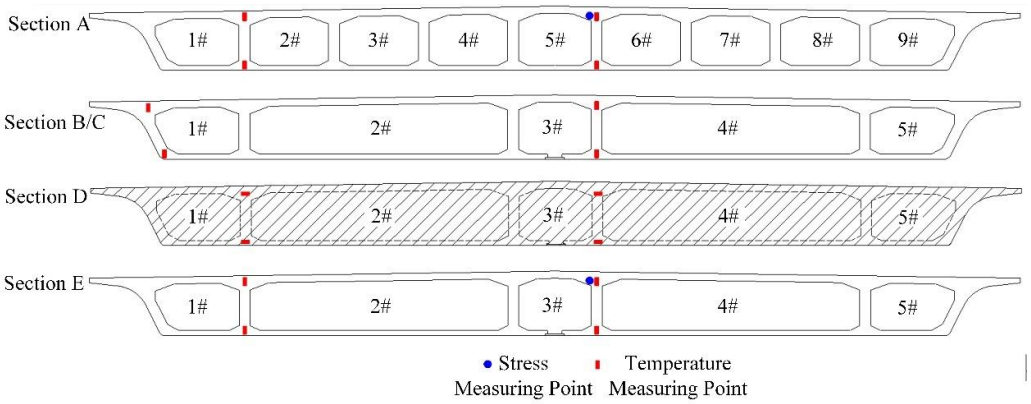

Fig.9 - Layout of stress and temperature measuring points of the main girder

Tower

The strain measuring points for the main tower are strategically positioned in three sections: at the base of the tower, 15.2 m above the main girder, and 16.5 m above the main girder. Sections H, I, and J represent the strain test sections of the main tower. The strain sensors for the main tower should be installed along the axis of the bridge tower. The arrangement of these measurement points is illustrated in Figure 10.

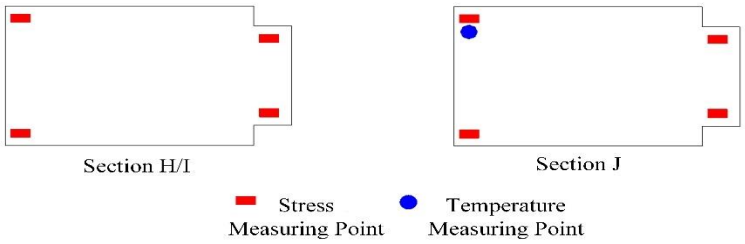

Fig.10 - Layout of tower stress and temperature measuring points

Arch rib

The steel box arch rib strain measurement points are arranged at the arch foot and mid-span position of 1# pier, and there are 2 sections in total. Sections F and G are designated as the strain test sections for the steel box arch rib. The strain sensors for the steel box arch rib should be installed along the length of the arch rib. The arrangement of the measurement points is depicted in Figure 11.

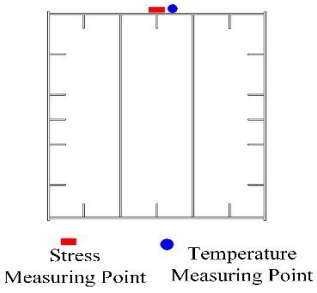

Fig.11- Layout of arch rib stress and temperature measurement points

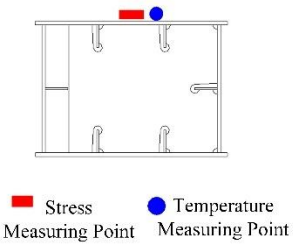

Fig.12 - Transverse brace stress and temperature measuring point layout

Wind bracing

The strain measuring point for the K-shaped transverse wind brace of the main arch rib is

positioned at the 3# wind brace, comprising a total of one section. The strain gauge is installed on the upper surface of the end of the arch rib, in proximity to the K-brace transverse brace. The arrangement of these measurement points is illustrated in Figure 12.

The embedded concrete strain gauge is used to monitor the stress of the main girder and tower, and the measured concrete strain is converted to the corresponding stress value. The JMT-36B temperature sensor was selected for temperature monitoring. In order to make the measurement results more accurate, the JM2X-212AT surface strain gauge is selected for steel structure strain monitoring. The layout and test conditions of field strain gauges and sensors are shown in Figure 13~ Figure 16.

Fig.13 - Main girder strain gauge installation diagram

Fig.14- Strain test diagram of main girder

Fig.15-Strain test diagram of bridge tower

Fig.16- Strain test diagram of arch rib

Structural elevation and cable force monitoring

The main girder, tower and arch rib elevation monitoring section is selected as the key section of construction. There are 13 main girder monitoring sections, 17 tower monitoring sections and 9 arch rib monitoring sections. The specific layout of the monitoring section is shown in Figure 17.

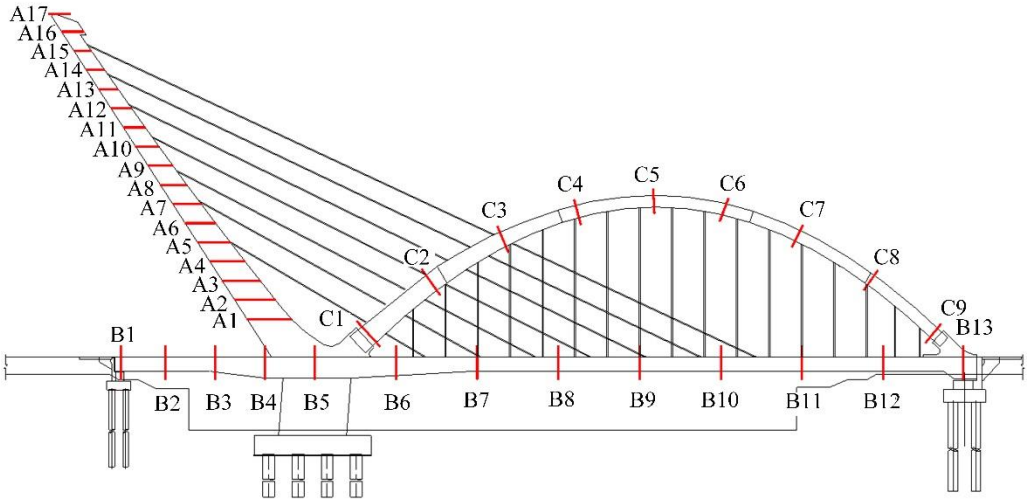

Fig.17- Elevation of linear monitoring section layout

Main girder elevation and center line deviation monitoring

A total of 13 sections of the main beam should be observed for the deviation of elevation and center line. Each section of the elevation observation point is arranged with 4 measuring points, which are corresponding positions on the outside of the anti-collision wall, and the deviation measuring points on the center line are corresponding bridge floor points on the center line of the box girder. The tasks of monitoring are as follows: measuring the elevation of the whole bridge during the main girder pouring, tower construction, triple tensioning of the stay cable, sling tensioning and completion of the bridge.

Main tower elevation monitoring

The measurement of the main tower's displacement involves determining the displacement value in both the longitudinal (along the bridge) and transverse (across the bridge) directions. The measuring points along the longitudinal direction are positioned at the interfaces of each section during the die-turning construction process. Additionally, measuring points are arranged on the side of the cable tower, close to the arch rib. The monitoring task entails measuring all elevations of the tower during various stages, including during the construction of the tower itself, during the three tensioning phases of the stay cables, during the tensioning of the boom, and upon the completion of the bridge. The monitoring tasks are as follows: all the elevations of the tower are measured during tower construction, stay cable tensioning, sling tensioning and bridge formation.

Arch rib elevation monitoring

Elevation observation points are strategically placed at various sections along both sides of the arch rib, including the arch foot, L/8, L/4, 3L/8, L/2, 5L/8, 3L/4, and 7L/8 sections. These measurement points are located on the sides of both the left and right arch ribs. The monitoring tasks associated with these points encompass the following: lifting of the arch rib, removal of arch rib supports, tensioning of slings, and monitoring of arch rib measurement points during the bridge stage. Figures 18 and 19 illustrate the calibration points of the main girder and the elevation of the tower, respectively.

Fig.18 -Main girder elevation measurement anchor point

Fig.19 -Tower elevation measurement diagram

BRIDGE CONSTRUCTION CONTROL EFFECT

Key construction control effect

To gain a comprehensive understanding of the actual stresses experienced by the bridge during construction, real-time monitoring is conducted on the stress and displacement of critical sections of the tower, arch rib, and main beam. Additionally, the stress of key sections of the wind bracing, as well as the internal forces of critical slings and stay cables, are also monitored. The measured data from these key construction stages are then analyzed.

Tower

Tower stress

Since the A1~A16 sections of the cable tower are all constructed by tilting mold, the cable force only balances the dead weight of the cable tower, especially when the cantilever length of the cable tower is long, the stress of the cable tower should be monitored. The comparisons between the measured and theoretical values of the left and right stresses in the tower test sections I, J, and H at each key construction stage are presented in Figures 20, 21 and 22.

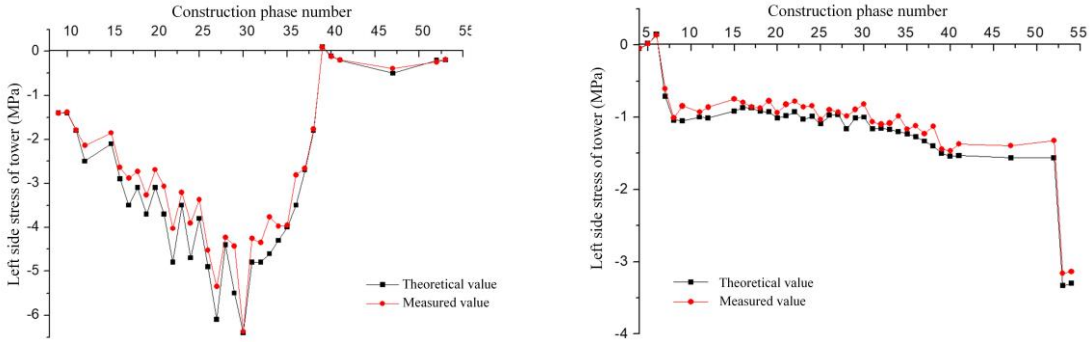

(a) Left side of the bridge tower *(b) Right side of the tower*

Fig.20 - The section I stress comparison during construction

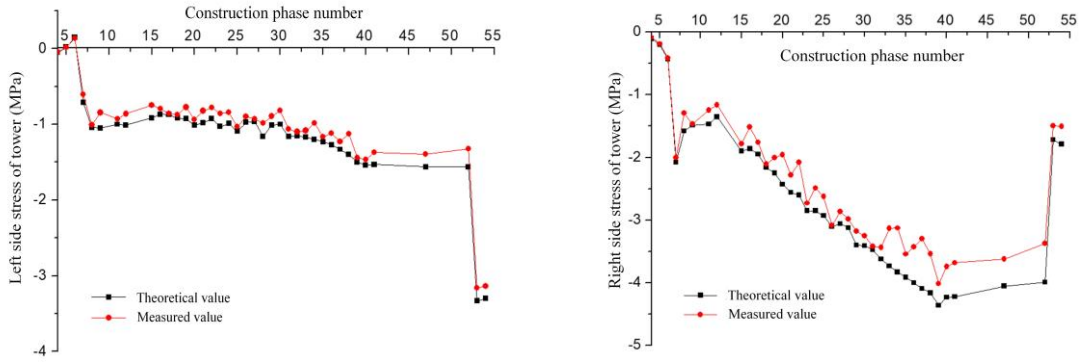

(a) Left side of the tower *(b) Right side of the tower*

Fig.21- Section J stress comparison during construction

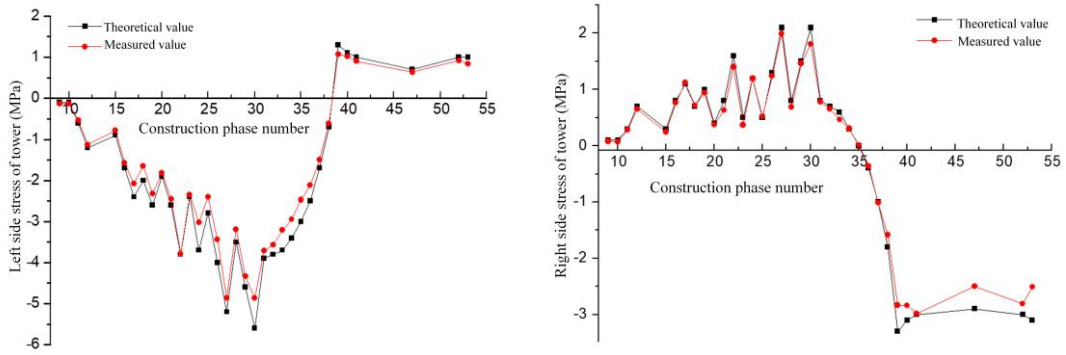

(a) Left side of the tower *(b) Right side of the tower*

Fig.22- The section H stress comparison during construction

As evident from Figures 20 to 22, the overall trend of the measured stress aligns with the theoretical stress. However, the measured stress values are lower than the theoretical ones, primarily due to the finite element model's inability to accurately simulate the behavior of ordinary steel bars. The stress on both the left and right sides of sections I and H gradually increases as construction progresses, peaking upon the completion of section A16 or section A14, respectively. Section I on the left is -5.6 MPa and Section I on the right is 2.3 MPa. The H section on the left is -4.9 MPa, and the H section on the right is 2.0 MPa. As construction progressed, the stress on the left side of section J of the tower girder gradually increased. Conversely, after the unloading of the main girder and tower support, the stress on the right side decreased. The maximum stress recorded on section J was -4.0 MPa. Notably, the stress levels in the tower conformed to the standard requirements.

During the cantilever construction of the tower, the maximum stress in the tower can be mitigated by tensioning the cable once per process. As the tensile force of the cable increases, the compressive stress on the left side of sections I and H gradually diminishes, potentially even transitioning into tensile stress. Meanwhile, the tensile stress on the right side progressively decreases, ultimately transforming into compressive stress. The stay cable plays a pivotal role in enhancing the structural forces during the mold construction process.

The tensile stress on the left side of the tower diminishes, while the compressive stress gradually increases. Conversely, the compressive stress on the right side of the tower decreases progressively. Because after the derrick is stretched, the main girder arches up, the extension of the cable decreases, and its internal force decreases.

Tower displacement

The junction node between S01 and the pylon is selected as the representative. The variables of the horizontal and vertical displacement of the pylon in the construction process are shown in Figure 23.

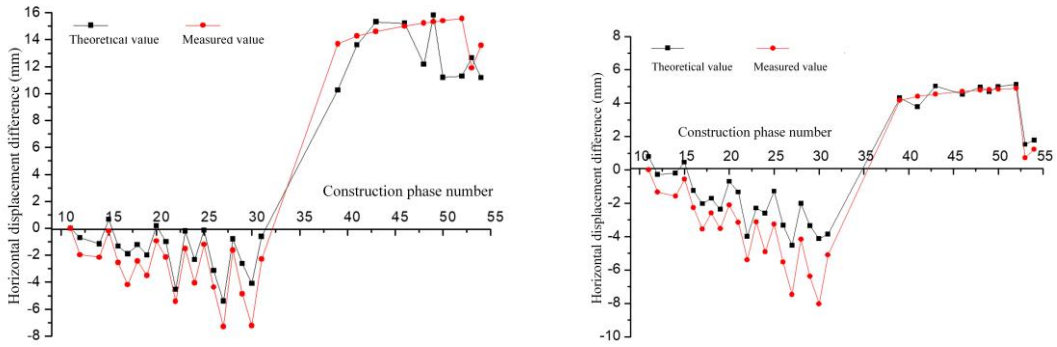

(a) Horizontal displacement difference *(b) Vertical displacement difference*

Fig.23 - The tower displacement difference comparison in each construction stage

As observed in Figure 23, the theoretical and measured values of tower displacement exhibit a similar overall trend. In the early stages, the measured values are smaller than the theoretical ones, although significant discrepancies arise between them in the later construction phases. As the cantilever length increases, both the horizontal and vertical displacements of the cable tower augment. However, the tension cable effectively mitigates these displacements. With an increase in the tension force of the cable, the direction of displacement in the cable tower shifts from the side with the smaller pile number towards the side with the larger pile number, and from downward displacement to upward displacement. Due to the self-balancing construction using tension cables, during the construction process, in order to remove the bottom support of the bridge tower, the tension force of the tension cables is used to balance the self-weight of the bridge tower. Therefore, during the tension stage of the tension cables, the bridge tower will experience significant horizontal and vertical displacements.

Main girder

Figure 24 presents a comparison between the measured and theoretical values of the stress measurement points for test section C, located in the middle span of the main girder, during certain key construction stages.

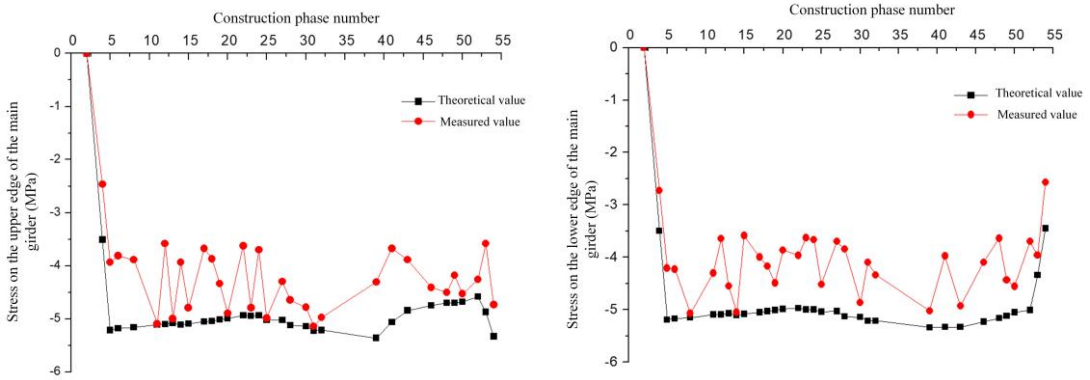

(a) Upper edge of main girder *(b) Lower edge of main girder*

Fig.24 - The section C stress comparison during construction

The measured stress values on both the upper and lower edges of the main beam closely align with the theoretical values, albeit being slightly smaller, as depicted in Figure 24. Throughout the construction process, the main girder span experiences compressive stress consistently. The maximum stress measured on the upper edge is -5.1 MPa, and similarly, the maximum stress measured on the lower edge is also -5.1 MPa; both of these values adhere to the code requirements. Given that the entire main beam is constructed with full support, the tension in the stay cable and derrick has a minimal impact on the stress distribution within the main beam. Upon unloading the main girder support, the compressive stress on the upper edge of the main girder intensifies, whereas the compressive stress on the lower edge decreases.

Arch rib stress

Figure 25 presents a comparison between the measured stress value and the theoretical stress value for test section G, located in the span of the arch rib, during a key construction stage.

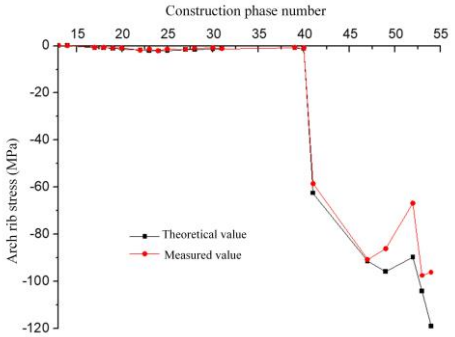

Fig.25 - The section G stress comparison during construction

As shown in Figure 25, the measured stress on the upper edge of the arch rib follows the overall trend of the theoretical value during construction, albeit being slightly smaller. Throughout the construction process, the middle and upper edges of the arch rib span experience compressive stress. Initially, due to the construction of the arch rib support, the stress in the arch rib remains low. However, upon unloading the arch rib support, the stress in the span of the arch rib increases rapidly. After the unloading of the main beam support, the measured stress attains its maximum value of -97.5 MPa, which complies with the code requirements.

Wind bracing stress

Figure 26 displays a comparison between the measured and theoretical stress values for section K during several key construction stages.

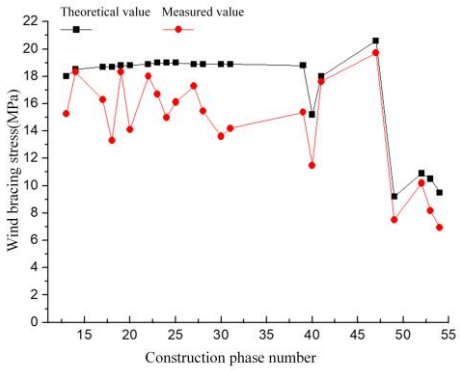

Fig. 26 - The K section stress comparison during construction

As illustrated in Figure 26, the measured stress value at the upper edge of the K brace exhibits an overall trend that is consistent with the theoretical value during construction. However, the measured value is slightly smaller than the theoretical value. The upper edge of the K-type support is in a tension state during the construction process, and the measured stress reaches the maximum value of 19.7 MPa after the tensioning of the derrick LX01, LX02, LX03, RX01, RX02, RX03, which meets the requirements of the specification.

Cable force test

The analysis of the measured cable forces for the stay cable S08 and the sling LD10 during the key construction process is presented in Figures 27 and 28, respectively.

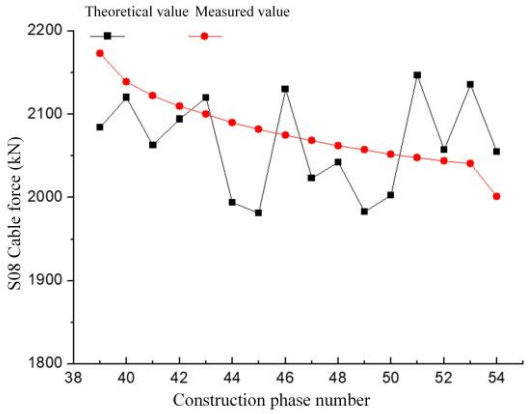

Fig.27 - S08 cable force comparison

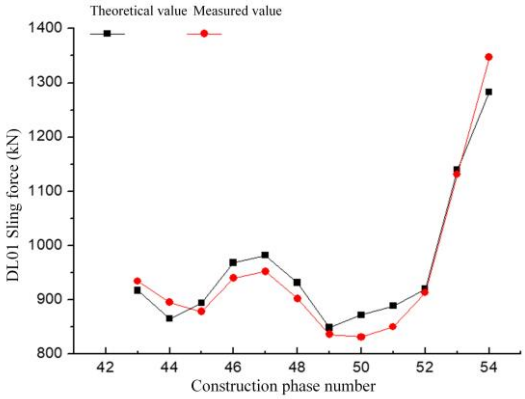

Fig.28 - LD10 cable force comparison

As observed in Figures 27 and 28, the overall trend of the measured cable forces closely aligns with the theoretical values. Specifically, the maximum discrepancies between the measured and theoretical values for the stay cable S08 and the suspension rod LD10 are 4.8% and -4.9%, respectively, both of which satisfy the specification requirements. Furthermore, the cable force of the stay cable S08 gradually diminishes as construction progresses, whereas the cable force of the suspension rod LD10 progressively increases with the advancement of construction.

Bridge state control effect

Elevation control

Based on the design elevations of the main girder, arch rib, and tower, along with the preset pre-arch degree, the corresponding vertical mold elevations are determined. The least squares method is employed to identify and adjust for any parameter errors that arise during the construction process, ensuring that the relevant lines adhere to the code requirements. The elevation errors for each key section of the bridge are depicted in Figure 29.

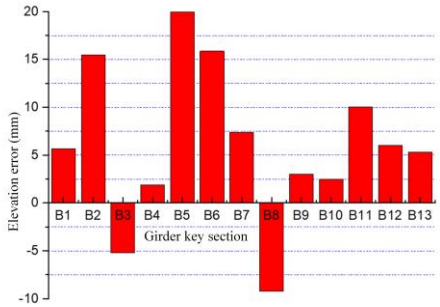

(a) Elevation error diagram of key section of main girder

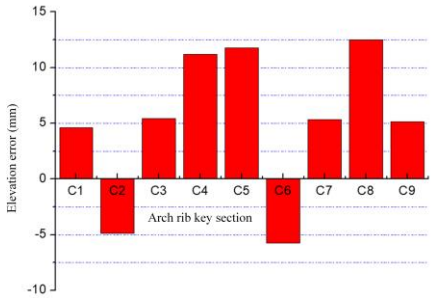

(b) Elevation errors of key sections of arch ribs

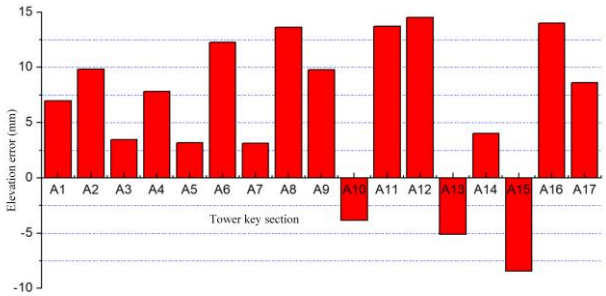

(c) Elevation error diagram of key sections of the main girder

Fig.29- Elevation errors of key sections

As illustrated in Figure 29, following the construction of the bridge deck pavement, railings, and other secondary loads, as well as the removal of the main beam supports, the elevation of the entire bridge falls within the error control range, satisfying both specification and design requirements. Specifically, the overall elevation of the main beam is slightly above the design value, with a maximum deviation of 20.0 mm. Similarly, the overall elevation of the arch rib and the cable tower are also slightly higher than their respective design elevations, with maximum deviations of 12.5 mm and 14.5 mm. These slight elevations are advantageous as they contribute to reducing prestress loss in the main beam and decreasing its deflection.

Stress control

By monitoring the stress value of each key surface in real time, the stress change and the final stress value can be fully controlled. The measured stress value of each stress control section in each construction stage does not exceed the limit, and the stress of the main beam, arch rib and cable tower in the bridge completion stage is shown in Figure 30.

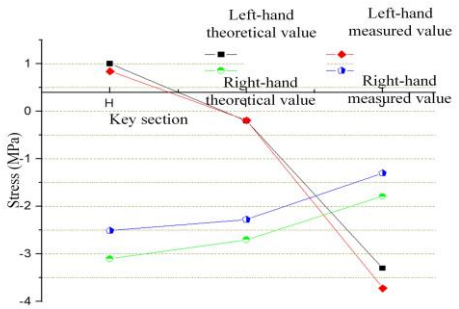

(a) Pylon control cross-section diagram

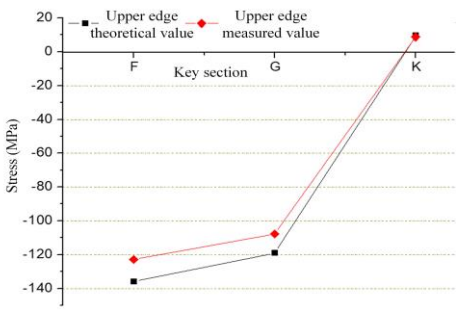

(b) Stress diagram of arch rib and wind support control section

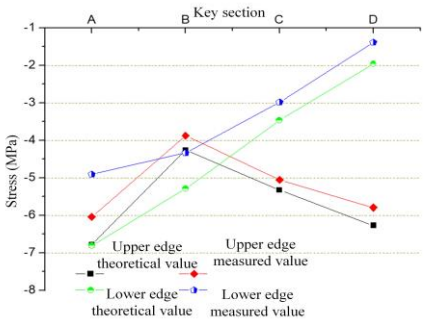

(c) Main girder control section diagram

Fig.30 -Stress diagram of each key section

As shown in Figure 30, the measured stress of each control section at the bridge completion stage is basically consistent with the theoretical stress. The upper edge of the arch rib, the main girder and the tower at the prestressed section are all under pressure, and the upper edge of the wind brace is subject to small tensile stress. At the height of 16.5 m above the bridge girder, the left side of the tower is strained and the right side is compressed, and the tensile stress is only 1.0 MPa, which indicates that the design is reasonable and the construction control measures are appropriate.

Cable force control

Since the cable of the bridge is divided into three tensioning times, the tensioning process is complicated, and the cable plays an important role in the stress of the tower construction process, so the cable force of the cable-stayed cable should be closely monitored, and the cable force of the remaining cable-stayed cable should be measured every time one cable is tensioned. This paper only analyzes the cable forces of the cable-stayed cable and boom when the bridge is completed, and the cable forces during the construction phase when the cable-stayed cable is fully tensioned, as shown in Figure 31 and Figure 32.

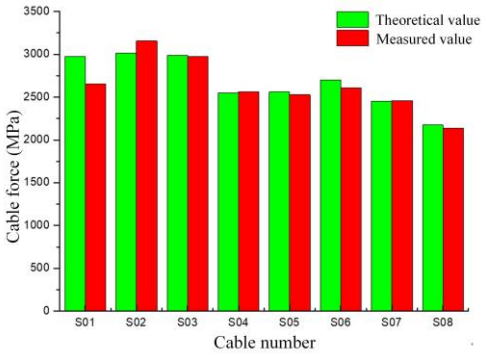

Fig.31- Cable force value of the cable during construction

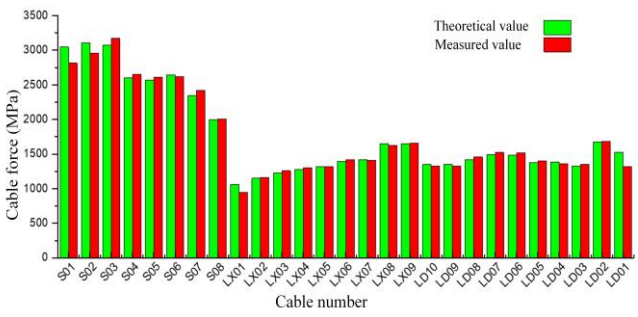

Fig.32- Bridge cable force value

As shown in Figures 31 and 32, the errors of short cable S01, LX01 and LD01 are relatively large, which are 7.6%, 10.9% and 13.4%, respectively. The errors of the remaining cable and derrick force are all within the range required by the specifications. This is because the short cable testing force is more obviously affected by the cable length error.

CONCLUSIONS

(1) The measured stress values on the upper and lower edges of the main girder align with the overall trend of the theoretical values, albeit being slightly smaller. Throughout the entire construction process, the main beam span experiences compressive forces. The measured maximum stress on the upper edge is -5.1 MPa, and similarly, the measured maximum stress on the lower edge is also -5.1 MPa. Both of these values comply with the code requirements.

(2) The elevation of the main girder is marginally higher than the design value, with a maximum deviation of 20.0 mm. Similarly, the overall elevation of the arch rib exceeds the design elevation slightly, with a maximum deviation of 12.5 mm. The tower's overall elevation is also slightly above the design elevation, with a maximum deviation of 14.5 mm. These slight elevations are advantageous as they contribute to minimizing prestress loss in the main girder and reducing its deflection.

(3) The upper edge of the arch rib, the main girder and the prestressed section tower are all under pressure, and the upper edge of the transverse brace is subjected to little tensile stress. At the height of 16.5 m above the bridge girder, the left side of the tower is strained and the right side is compressed, and the tensile stress is only 1.0MPa, which indicates that the design is reasonable and the construction control measures are appropriate.

REFERENCES

[1] Puri N, Turkan Y. Bridge construction progress monitoring using lidar and 4D design models[J]. Automation in Construction, 2020, 109: 102961.

[2] He Z, Li W, Salehi H, et al. Integrated structural health monitoring in bridge engineering[J]. Automation in construction, 2022, 136: 104168.

[3] Jiang Z, Shen X, Ibrahimkhil M H, et al. Scan-vs-BIM for real-time progress monitoring of bridge construction project[J]. ISPRS Annals of the Photogrammetry, Remote Sensing and Spatial Information Sciences, 2022, 10: 97-104.

[4] Tian J, Luo S, Wang X, et al. Crane lifting optimization and construction monitoring in steel bridge construction project based on BIM and UAV[J]. Advances in Civil Engineering, 2021, 2021(1): 5512229.

[5] Lin Y B, Pan C L, Kuo Y H, et al. Online monitoring of highway bridge construction using fiber Bragg grating sensors[J]. Smart Materials and Structures, 2005, 14(5): 1075.

[6] Bai Y, Huan J, Kim S. Measuring bridge construction efficiency using the wireless real-time video monitoring system[J]. Journal of Management in Engineering, 2012, 28(2): 120-126.

[7] Fujino Y, Siringoringo D M. Bridge monitoring in Japan: the needs and strategies[J]. Structure and Infrastructure Engineering, 2011, 7(7-8): 597-611.

[8] Zhou G D, Yi T H, Li W J, et al. Standardization construction and development trend of bridge health monitoring systems in China[J]. Advances in Bridge Engineering, 2020, 1: 1-18.

[9] Butler L J, Lin W, Xu J, et al. Monitoring, modeling, and assessment of a self-sensing railway bridge during construction[J]. Journal of Bridge Engineering, 2018, 23(10): 04018076.

[10] Fu M, Liang Y, Feng Q, et al. Research on the application of multi-source data analysis for bridge safety monitoring in the reconstruction and demolition process[J]. Buildings, 2022, 12(8): 1195.

[11] Kim H, Moon B, Hu X, et al. Construction and performance monitoring of innovative ultra-high-performance concrete bridge[J]. Infrastructures, 2021, 6(9): 121.

[12] Xin J, Wang C, Tang Q, et al. An evaluation framework for construction quality of bridge monitoring system using the DHGF method[J]. Sensors, 2023, 23(16): 7139.

[13] Wan B. Using fiber-reinforced polymer (FRP) composites in bridge construction and monitoring their performance: an overview[J]. Advanced composites in bridge construction and repair, 2014: 3-29.

[14] Gou H, Liu C, Bao Y, et al. Construction monitoring of self-anchored suspension bridge with inclined tower[J]. Journal of Bridge Engineering, 2021, 26(10): 05021011.

[15] Fang Y M, Chou T Y, Hoang T V, et al. Automatic management and monitoring of bridge lifting: a method of changing engineering in real-time[J]. Sensors, 2019, 19(23): 5293.

[16] Yang H, Xia M. Advancing bridge construction monitoring: AI-based building information modeling for intelligent structural damage recognition[J]. Applied Artificial Intelligence, 2023, 37(1): 2224995.

[17] Xin J, Jiang Y, Wu B, et al. Intelligent Bridge Health Monitoring and Assessment[J]. Buildings, 2023, 13(7): 1834.